Published online 13 October 2014 *Nucleic Acids Research, 2014, Vol. 42, No. 20* **12899–12911**
doi: 10.1093/nar/gku942

Suppression of subtelomeric VSG switching by *Trypanosoma brucei* TRF requires its TTAGGG repeat-binding activity

Sanaa E. Jehi[1,†], Xiaohua Li[2,3,†], Ranjodh Sandhu[1,‡], Fei Ye[4,‡], Imaan Benmerzouga[1], Mingjie Zhang[4], Yanxiang Zhao[2,*] and Bibo Li[1,5,6,7,*]

[1]Center for Gene Regulation in Health and Disease, Department of Biological, Geological, and Environmental Sciences, Cleveland State University, Cleveland, OH 44115, USA, [2]Department of Applied Biology and Chemical Technology, State Key Laboratory of Chirosciences, The Hong Kong Polytechnic University, Hung Hom, Kowloon, Hong Kong, P. R. China, [3]The Hong Kong Polytechnic University Shenzhen Research Institute, Shenzhen, P.R. China, [4]Division of Life Science, State Key Laboratory of Molecular Neuroscience, The Hong Kong University of Science and Technology, Clear Water Bay, Kowloon, Hong Kong, P. R. China, [5]Case Comprehensive Cancer Center, Case Western Reserve University, Cleveland, OH 44106, USA, [6]Department of Molecular Genetics, Cleveland Clinic Lerner Research Institute, Cleveland, OH 44195, USA and [7]The Rockefeller University, New York, NY 10065, USA

Received June 05, 2014; Revised September 24, 2014; Accepted September 27, 2014

ABSTRACT

***Trypanosoma brucei* causes human African trypanosomiasis and regularly switches its major surface antigen, VSG, in the bloodstream of its mammalian host to evade the host immune response. VSGs are expressed exclusively from subtelomeric loci, and we have previously shown that telomere proteins *Tb*TIF2 and *Tb*RAP1 play important roles in VSG switching and *VSG* silencing regulation, respectively. We now discover that the telomere duplex DNA-binding factor, *Tb*TRF, also plays a critical role in VSG switching regulation, as a transient depletion of *Tb*TRF leads to significantly more VSG switching events. We solved the NMR structure of the DNA-binding Myb domain of *Tb*TRF, which folds into a canonical helix-loop-helix structure that is conserved to the Myb domains of mammalian TRF proteins. The *Tb*TRF Myb domain tolerates well the bulky J base in *T. brucei* telomere DNA, and the DNA-binding affinity of *Tb*TRF is not affected by the presence of J both *in vitro* and *in vivo*. In addition, we find that point mutations in *Tb*TRF Myb that significantly reduced its *in vivo* telomere DNA-binding affinity also led to significantly increased VSG switching frequencies, indicating that the telomere DNA-binding activity is critical for *Tb*TRF's role in VSG switching regulation.**

INTRODUCTION

Trypanosoma brucei (*T. brucei*) is a protozoan parasite that causes human African trypanosomiasis, which can be fatal if left untreated. Current available drugs treating *T. brucei* infection have severe side effects, and incidents of drug resistance have been increasingly observed (1), making it imperative to develop new generation anti-trypanosome drugs. Bloodstream form (BF) *T. brucei* regularly switches its major surface antigen, variant surface glycoprotein (VSG), inside its mammalian host to evade the host immune response (2). This antigenic variation is a key pathogenesis mechanism essential for a long-term *T. brucei* infection.

T. brucei has more than 2000 *VSG* genes and pseudogenes in its genome, mostly clustered at subtelomeric regions (3,4). However, VSGs are exclusively expressed from *VSG* expression sites (ESs) in a monoallelic fashion. BF *VSG* ESs are polycistronic transcription units (PTUs) transcribed by RNA polymerase I (5) and are located immediately upstream of the telomere (6). In the *T. brucei* Lister 427 strain used in this study, 15 ESs have been identified, all of which have highly conserved DNA sequences (90% identical) and gene organizations (7). *VSG* is always the last gene in any ES, located within 2 kb from the telomere repeats, while the ES promoter is 40–60 kb upstream (7,8). At any moment, only one ES is fully active, resulting in a single type of VSG being expressed. This monoallelic *VSG* expres-

*To whom correspondence should be addressed. Tel: +1 216 687 2444; Fax: +1 216 687 6972; Email: b.li37@csuohio.edu
Correspondence may also be addressed to Yanxiang Zhao. Tel: +852 3400 8706; Fax: +852 2364 9932; Email: yanxiang.zhao@polyu.edu.hk
†The authors wish it to be known that, in their opinion, the first two authors should be regarded as Joint First Authors.
‡These authors contributed equally to the paper as second authors.

sion ensures that the previously active VSG is no longer expressed after a VSG switching event, which is essential for the effectiveness of antigenic variation.

VSG switching has several major pathways (9). In *in situ* switching, the originally active ES is silenced while an originally silent one is expressed without DNA rearrangements. Other major VSG switching pathways are homologous recombination- (HR-) mediated. In crossover (CO) events, part of the active ES, including the *VSG* gene, changes place with that of a silent ES without losing any genetic information. In gene conversion (GC) events, a silent *VSG* is copied into the active ES to replace the active *VSG* gene, resulting in the loss of the originally active *VSG* and duplication of the newly active *VSG*. GC is the preferred mechanism of VSG switching in the Lister 427 strain used in this study (9). It can encompass only the *VSG* gene and its neighboring regions (termed *VSG* GC) or the entire ES (termed ES GC). In addition, the entire active ES can be lost, and an accompanying *in situ* switch can give rise to ES loss + *in situ* switchers (10–12). Several proteins involved in HR have been shown to play important roles in VSG switching: deletion of *Tb*RAD51, *Tb*RAD51-3 or *Tb*BRCA2 leads to decreased VSG switching frequencies (13–15). In contrast, deletion of TOPO3α and RMI1 leads to more frequent VSG switching (11,16).

The *T. brucei* telomere has been implicated in the regulation of VSG expression and switching (17). We have previously shown that a telomere protein, *Tb*RAP1, is required for silencing subtelomeric *VSGs* (18,19). We have recently shown that another telomere protein, *Tb*TIF2, is important for maintaining subtelomere/telomere integrity, and depletion of *Tb*TIF2 led to elevated VSG switching frequencies (12). Therefore, telomere proteins are important for regulation of *VSG* expression and VSG switching. A study by Hovel-Miner *et al*. showed that *T. brucei* cells carrying extremely short telomeres (∼1.5 kb) exhibited an ∼10-fold higher VSG switching frequency when compared to cells with longer telomeres of 15 kb on average (20), indicating that the telomere structure indeed plays an important role in VSG switching regulation.

Our previous study identified a duplex telomere DNA-binding factor, *Tb*TRF, which interacts with both *Tb*RAP1 (18) and *Tb*TIF2 (12). While *Tb*TRF is essential for maintaining the terminal telomere structure (21), it does not affect ES-linked *VSG* silencing in BF *T. brucei* cells (18). It is intriguing whether *Tb*TRF plays any important role in VSG switching regulation. *Tb*TRF has a similar domain structure as mammalian duplex telomere DNA-binding factors TRF1 and TRF2, with an N-terminal TRF Homology (TRFH) domain and a C-terminal Myb domain based on sequence analysis (21). In mammalian TRF1 and TRF2, the TRFH domain is required for homodimerization of these factors that serve as an interaction platform to bind other telomeric proteins including TIN2 and Apollo (22). The Myb domain specifically binds to telomeric TTAGGG repeats and serves to package both TRF1/2 and their binding partners onto the telomere to form an integrated protective structure (23–25). While our study has shown that *Tb*TRF has a strong duplex TTAGGG repeat binding activity (21), it remains to be confirmed whether its C-terminal Myb domain mediates this direct interaction. Furthermore, whether the Myb-mediated DNA-binding activity of *Tb*TRF exerts any impact on VSG regulation is completely unknown.

Another interesting aspect regarding *Tb*TRF and VSG regulation involves the base J. In kinetoplastids, a heavily modified base β-D-glucosyl(hydroxymethyl)uracil, J, has been identified to replace a small fraction of thymidines in the genome (26,27). J is only present in the BF *T. brucei* DNA but not in the DNA of procyclic form (PF) *T. brucei* cells that normally reside in the mid-gut of their insect vector, tsetse (*Glossina spp.*) (26). A relatively high level of J is found in *T. brucei* telomeric DNA. Fourteen percent of the T in the $(CCCTAA)_n$ strand and 36% of T in the $(TTAGGG)_n$ strand is replaced by J (28). Silent *VSG* ESs contain J, while the active ES does not (29). In addition to its presence in the telomere, J appears to be also enriched at tandem repeat regions of *T. brucei* genome (30). Furthermore, recent studies also showed that a small amount of J is located at regions flanking RNA polymerase II (RNAP II) PTUs throughout the *T. brucei* genome (31).

J's function appears to be species-specific in kinetoplastids. In *T. brucei*, J seems to be involved in regulation of transcription elongation within certain RNAP II PTUs (32). In *Trypanosoma cruzi* that causes Chagas disease, J is located at the transcription initiation sites of RNAP II PTUs, and loss of J led to elevated RNAP II transcription (33). In *Leishmania major* that causes leishmaniasis, J is located at the transcription termination sites of RNAP II PTUs, and loss of J led to readthrough of RNAP II-mediated transcription (32,34). With the enrichment of base J in *T. brucei* telomeric DNA, it is intriguing whether the DNA-binding Myb domain of *Tb*TRF would interact with J-containing TTAGGG repeats any differently from regular sequences. Furthermore, whether such differences would have any implication on VSG regulation is worth investigating.

To address these questions, we conducted a series of structural and functional studies on the Myb domain of *Tb*TRF. The structure of the *Tb*TRF Myb domain was determined by nuclear magnetic resonance (NMR). The DNA-binding activity of *Tb*TRF, particularly the interaction between *Tb*TRF and J-containing TTAGGG sequence, was characterized by *in vitro* binding assays and *in vivo* Chromatin Immunoprecipitation (ChIP) experiments. Structure-based mutational analysis identified a few residues critical for Myb domain folding and its binding to telomere. We found that a transient depletion of *Tb*TRF led to a 6-fold increase in VSG switching frequency. More importantly, *Tb*TRF Myb domain mutations that significantly decreased *Tb*TRF's association with the telomeric DNA *in vivo* also caused significantly more frequent VSG switching events, indicating that the telomere DNA-binding activity of *Tb*TRF plays an important role in VSG switching regulation.

MATERIALS AND METHODS

VSG switching assay

VSG switching frequencies in S/TRFi clones B1, A7 and A8 were first determined by a method without enrichment of switchers through magnetic-activated cell sorting (MACS) column as described in (12).

The improved VSG switching assay enriches switchers by passing cells through MACS column that binds a VSG2 monoclonal antibody (20). Detailed protocol can be found in the supplemental materials.

ChIP

ChIP was performed as described in (35).

Quantitative reverse transcriptase-polymerase chain reaction

Quantitative RT-polymerase chain reaction (qRT-PCR) was performed the same way as described in (12).

Electrophoresis mobility shift assay

Double-stranded oligos were prepared by standard annealing process after the two single-stranded DNA molecules were mixed in equal molar ratio. The annealed double-stranded oligos were then purified by gel electrophoresis before used in electrophoresis mobility shift assay (EMSA) or NMR experiments. The regular or J-containing DNA (25 pmol) was incubated with increasing amount of *Tb*TRF Myb protein (0, 25, 50, 60, 75, 100, 120 or 130 pmol) in buffer containing 20 mM HEPES pH 7.5, 40 mM KCl, 10 mM $MgCl_2$, 10 mM $CaCl_2$, 10 mM β-mercaptoethanol, 0.25 mg/ml bovine serum albumin, 8% (v/v) glycerol at 4°C for 5 h and 37°C for 15 min immediately before subjected to 5% native polyacrylamide gel and run at 150 V in 0.25 × TBE buffer at 4°C for 2 h. Gels were stained by EtBr and scanned by ChemiDoc™ XRS Imager (BioRad).

Protein expression and purification

The Myb domain of *Tb*TRF (residues 281–382) was cloned as a His_6-tagged protein in a modified pET32 vector containing the human rhinovirus (HRV) 3C protease cleavage site and without thioredoxin fusion. The mutants (R298K, R298E, Q320S, Q321S, H346R, R348K, R348E and R352K) were generated by site-directed mutagenesis (Finnzyme) and cloned into the same vector as wild-type *Tb*TRF. Wild-type and mutant *Tb*TRF Myb domain constructs were expressed in *Escherichia coli* BL21 (DE3) cells at 25°C for 8 h after induction by isopropyl-β-D-thiogalactopyranoside at 0.75 mM concentration. Target proteins were purified by affinity chromatography (HisTrap HP, GE Healthcare). The His_6 tag was removed by 3C cleavage and the untagged protein was further purified by size-exclusion chromatography (Superdex 75, GE Healthcare).

NMR spectroscopy

The protein samples for NMR studies were concentrated to ∼0.2 mM for titration experiments and ∼1.0 mM for structural determinations in 100 mM potassium phosphate at pH 5.8. NMR spectra were acquired at 10°C on Varian Inova 500 or 750 MHz spectrometers. For titration experiments, DNA oligos at 50 μM were added into the protein sample. Backbone and side chain resonance assignments were achieved by combination of standard heteronuclear correlation experiments including HNCO, HNCACB, CBCA(CO)NH and HCCH-TOCSY using $^{15}N/^{13}C$-labeled protein samples, and ^{1}H 2D TOCSY and NOESY experiments (36–38). Approximate interproton distance restraints were derived from 2D ^{1}H-NOESY, 3D ^{15}N-seperated NOESY and 3D ^{13}C-seperated NOESY spectra. Structures were calculated using the program CNS (39). Statistics were summarized in Supplementary Table S1. The coordinates of *Tb*TRF Myb domain have been deposited to Protein Data Bank (PDB ID 2M9H). The structure figures were prepared using the CCP4mg package (40) in CCP4.

Isothermal titration calorimetry

Isothermal titration calorimetry (ITC) was performed using an iTC200 microcalorimeter (MicroCal Inc.) as described previously (41–44). Additional details can be found in Supplemental Materials.

Synthetic J-DNA oligos

The J-containing oligos are purchased from Fidelity Systems Inc. (http://www.fidelitysystems.com/).

Pulsed field gel electrophoresis

Pulsed field gel electrophoresis (PFGE) was performed as described in (12).

RESULTS

Depletion of *Tb*TRF increases VSG switching frequency and changes VSG switching pattern

We previously found that *Tb*TRF plays an essential role in maintaining the telomere terminal structure (21), but does not seem to affect subtelomeric *VSG* silencing (18). However, whether *Tb*TRF plays any role in VSG switching regulation is unknown. To test this possible function of *Tb*TRF, we introduced the pZJMβ-based (45) *Tb*TRF RNAi construct (21) into the HSTB261 cells developed for VSG switching assays (16) to establish S/TRFi strains (S for switching). As expected, induction of *Tb*TRF RNAi by doxycycline in S/TRFi cells led to a cell growth arrest by 24 h (Figure 1A, Supplementary Figure S1A) and a decrease in *Tb*TRF protein level (Figure 1B, Supplementary Figure S1B).

In HSTB261, a *blasticidin-resistance* gene (*BSD*) was targeted immediately downstream of the active ES promoter, and a *puromycin-resistance* gene (*PUR*) fused with a *Herpes simplex* virus *thymidine kinase* (*TK*) gene was inserted between the 70 bp repeats and the *VSG2* gene in the same active ES (Supplementary Figure S1C) (16). *T. brucei* cells expressing *TK* are sensitive to ganciclovir (GCV), a nucleoside analog (46). Essentially all VSG switchers will lose the *PUR-TK* expression and become GCV resistant. Therefore, VSG switchers can be easily selected by GCV resistance. Because depletion of *Tb*TRF leads to a cell growth arrest (21), we induced the *Tb*TRF RNAi for a short period of time to enable subsequent recovery of VSG switchers. We found that induction of *Tb*TRF RNAi for 24 h followed by removal of doxycycline led to a depletion of *Tb*TRF protein

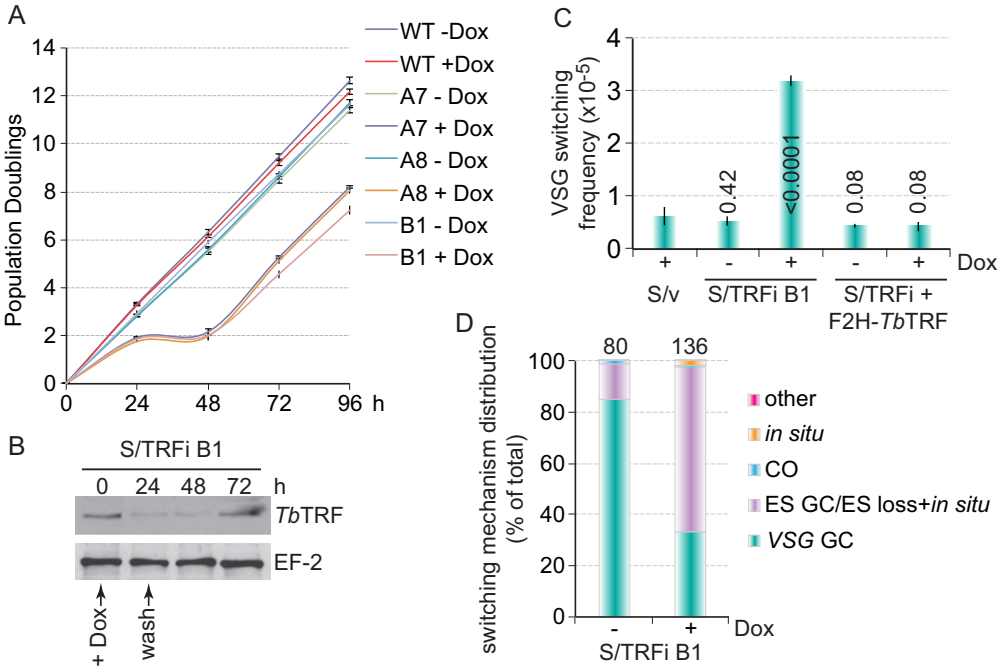

Figure 1. A transient depletion of *Tb*TRF led to an elevated VSG switching frequency. (**A**) S/TRFi cells experienced a transient growth arrest upon induction of *Tb*TRF RNAi by 100 μg/ml doxycycline for 24 h. Growth curves were calculated from three independent experiments. A7, A8 and B1 are independent S/TRFi clones. In this and other figures, error bars represent standard deviation. (**B**) *Tb*TRF protein level decreased upon induction of *Tb*TRF RNAi for 24 h. Western blotting was performed using whole cell lysate prepared from S/TRFi clone B1 cells and *Tb*TRF (21) and EF-2 (Santa Cruz Biotechnology, Inc.) antibodies. (**C**) VSG switching frequencies in S/v, S/TRFi B1 and S/TRFi+F2H-*Tb*TRF cells with or without a transient *Tb*TRF RNAi induction. Average switching frequencies were calculated from at least three independent switching assays. Numbers on columns indicate *P* values (unpaired *t* tests) when compared to the switching frequency in S/v cells. A *P* value less than 0.05 is considered significantly different. (**D**) VSG switching mechanism distribution in S/TRFi B1 cells under the induced and uninduced conditions. The total number of switchers characterized is indicated above each column. GC, gene conversion; CO, crossover.

and a growth arrest for 24 h followed by a recovery of the *Tb*TRF protein level and the growth (Figure 1A and B). The recovered *Tb*TRF RNAi cells exhibited growth arrest again when induced by doxycycline repetitively (Supplementary Figure S1A), indicating that the recovered population retained the ability of RNAi induction.

Before the VSG switching assay, cells were kept under selection with blasticidin and puromycin to ensure uniform expression of VSG2 in the population. At the beginning of the VSG switching assay, blasticidin and puromycin were removed from the medium to allow switchers to arise. Three independent S/TRFi clones were incubated with or without doxycycline for 24 h followed by removal of doxycycline by extensive cell washing and cell recovery. Induced S/TRFi cells typically took ∼48 h to fully recover, while the uninduced cells grew normally. Eventually, all cells were grown for the same number of population doublings to allow a fair comparison of VSG switching frequencies between induced and uninduced cells. A small fraction of cells was plated in the absence of GCV to determine the plating efficiency. Initially, we plated 0.5 million cells after each switching assay and found that a transient depletion of *Tb*TRF led to a significant increase in the VSG switching frequency (Supplementary Figure S1D, S1E), indicating that *Tb*TRF suppresses VSG switching.

We attempted to isolate sufficient switchers from S/TRFi cells to determine the VSG switching mechanisms. However, this original switching method is very inefficient and we could only obtain limited number of switchers in each assay. We therefore adopted the modified switching assay by enriching switchers using MACS beads that bind a monoclonal VSG2 antibody (20). Cells expressing VSG2 were retained by the MACS column, while switchers were enriched in the flow-through fraction and were plated in the presence of GCV for subsequent selection. This modified switching method allowed us to isolate ∼100 switchers under each condition, which greatly increased the assay efficiency. Using the MACS switching assay, we examined the VSG switching frequencies and mechanisms in HSTB261 cells carrying an empty RNAi vector (S/v) (12) and S/TRFi clone B1 cells under induced and uninduced conditions. We grew cells for approximately the same number of population doublings in both the original and the MACS switching assays to ensure that the results were comparable. We confirmed that a transient depletion of *Tb*TRF led to a 6-fold higher VSG switching frequency than that in S/v cells, while uninduced S/TRFi cells exhibited a similar VSG switching frequency as S/v cells (Figure 1C, Supplementary Figure S1F). S/v cells had a similar VSG switching frequency as reported in HSTB261 cells (11,16). Inducing the expression of an ectopic F2H-tagged WT *Tb*TRF allele in S/TRFi cells (Supplementary Figure S1H) also complemented the slow growth (Supplementary Figure S1G) and the elevated VSG switching frequency phenotypes (Figure 1C). Therefore, WT *Tb*TRF suppresses subtelomeric VSG switching. Our previous study showed that *Tb*TRF depletion did not

shorten telomere length dramatically (21). We confirmed that telomere length did not change significantly within the short frame of time when *Tb*TRF was depleted (Supplementary Figure S1I), indicating that elevated VSG switching frequency is not due to extremely short telomere lengths. However, extremely short telomere would presumably bind very few *Tb*TRF proteins, which would in turn result in increased VSG switching frequency, as observed in telomerase null cells with short telomeres (20).

Using the MACS switching assay, we obtained ∼100 or more VSG switchers under each assay condition. Analyzing a larger number of VSG switchers allowed us to reveal the typical VSG switching patterns more accurately. By characterizing the genotype and marker expression status, we can determine the VSG switching mechanisms (Supplementary Figure S1C) as described previously (11,12,16). By selecting switchers with various antibiotics and PCR analyses using *VSG*- or *BSD*-specific primers, we determined that before *Tb*TRF RNAi induction, most switchers (∼85%) were *VSG* GC events, while a considerable number of switchers were ES GC or ES loss + *in situ* events (∼14%) (Figure 1D). In contrast, after a transient depletion of *Tb*TRF, ES GC/ES loss + *in situ* events became predominant (65%), while only ∼33% of all switchers were *VSG* GC events (Figure 1D). In addition, *in situ* switchers were extremely rare in uninduced S/TRFi cells (none in examined *VSG* switchers), but increased to 1.5% in *Tb*TRF-depleted cells. Therefore, *Tb*TRF influences the VSG switching mechanisms.

The Myb domain of *Tb*TRF adopts the canonical helix-turn-helix structure

*Tb*TRF binds to the duplex TTAGGG telomere repeats directly (21). This affinity has been assigned to its C-terminal region that shares high sequence similarity to the Myb domains in mammalian TRF proteins (47). Myb domains are small structural modules of 50–60 residues that are commonly found in DNA-binding proteins (48). The structures of mammalian TRF Myb domains reveal a conserved fold of three-helix bundle with the classical helix-turn-helix motif as the DNA-binding element (23,49,50).

To further delineate the role of the *Tb*TRF Myb domain in VSG switching regulation, we first solved the NMR structure of this region. While the core region of the Myb domain consists of only 50–60 residues, a longer construct of *Tb*TRF Myb extending about 20 residues more on both the N- and C-termini is necessary to yield soluble protein. The heteronuclear single quantum correlation (HSQC) spectrum of ^{15}N-labeled *Tb*TRF Myb domain showed an excellent dispersion pattern typical of a well-folded protein (Figure 2A). The structure was determined with a conventional multidimensional heteronuclear NMR method with the statistics summarized in Supplementary Table S1. The final 20 structures superimpose well, with root-mean-square deviation (RMSD) of 0.6 Å for the backbone atoms in the core region (Figure 2B). The N- and C-terminal extensions, while critical for solubility of this domain, are highly flexible as they show few medium- and long-range nuclear overhauser effect signals.

The overall structure of *Tb*TRF Myb domain follows the canonical three-helix bundle architecture, with the second and third helix forming the helix-turn-helix motif for DNA binding. This *Tb*TRF Myb structure is very similar to the human TRF1 and TRF2 Myb structures, especially the three core helices with RMSD of 0.6 and 0.83 Å, respectively (Figure 2C). However, the loops connecting these helices adopt quite different conformations in *Tb*TRF from that of human TRF1 and TRF2, probably due to their intrinsic flexibility (Figure 2C).

*Tb*TRF Myb is stabilized by an extensive hydrophobic core consisting of a few conserved residues including I309, L313, L343 and W347 when compared to mammalian TRFs (Figure 2D). Another interesting observation about *Tb*TRF Myb is the pH sensitivity of its folding. The HSQC spectrum showed significant deterioration when buffer pH was adjusted from 5.8 to 6.5 (data not shown). Close inspection of the structure revealed that H346, the only residue in *Tb*TRF Myb with its imidazole side chain of pK_a around 6.5, is likely the major factor for this pH sensitivity. H346, located on the third helix, forms a salt bridge interaction with D306 on the first helix (Figure 2D). This interaction is critical for packing of these two helices to form the three-helix bundle. Deprotonation of H346 when buffer pH arises above 6.5 likely weakens this interaction and may lead to partial unfolding of *Tb*TRF Myb.

*Tb*TRF Myb domain binds to both regular and J-containing telomeric DNA

The direct interaction of the *Tb*TRF Myb domain with telomeric DNA repeats was first characterized by EMSA. Purified *Tb*TRF Myb peptide readily formed a complex with a 'double-repeat' DNA oligo that contained two telomeric repeats (5′ GGCGCGCTTAGGGTTAGGGTTACCGCCCG 3′) (Supplementary Figure S2A). We also used ITC to directly measure the binding affinity (K_d) between *Tb*TRF Myb and its DNA substrate. Our data showed that *Tb*TRF Myb bound to single- (5′ GGGGCCTTTAGGGTTATCCGCC 3′) and double-repeat (same sequence as used in EMSA) DNA oligos with comparable affinities at K_d of ∼20 μM (Figure 3A, Supplementary Figure S2B). In summary, these biochemical data confirm that *Tb*TRF Myb can directly bind to telomeric TTAGGG repeats.

A considerable amount of thymidine in the BF *T. brucei* telomeric DNA is replaced by the base J (28). J is absent in the PF *T. brucei* DNA, and *Tb*TRF associates with telomeric DNA in both BF and PF cells (21), indicating that the *Tb*TRF DNA-binding activity is not abolished by J or requires J. However, it is unknown whether the *Tb*TRF Myb domain binds J-containing telomeric DNA the same way as it binds the regular telomeric sequence.

To directly test whether J affects the DNA-binding activity of the *Tb*TRF Myb domain, we first constructed a synthetic J-containing duplex oligo with the sequence of TJAGGG/AATCCC to represent a single-repeat DNA substrate. The presence of J in this oligo was confirmed by mass spectroscopy (Supplementary Figure S3A). ITC analysis revealed that the binding affinity (K_d) of *Tb*TRF Myb to the J-containing oligo is ∼12 μM, comparable to that of the regular TTAGGG oligo (Figure 3A).

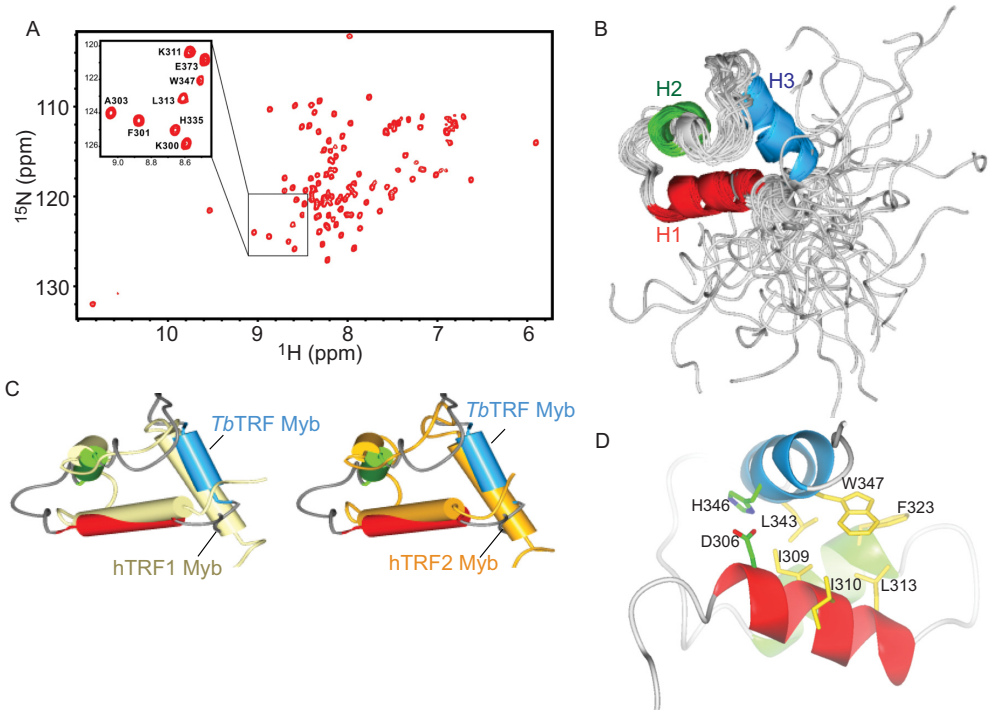

Figure 2. Structure of *Tb*TRF Myb domain. (**A**) The ^{1}H-^{15}N HSQC spectrum of ^{15}N-labeled *Tb*TRF Myb domain at pH 5.8. A selected region of the spectrum enclosed by a framed rectangle is expanded to show the detail of residue assignments. (**B**) Ensemble of the final 20 lowest energy structures of *Tb*TRF overlaid on the backbone. The three helices H1–H3 are drawn as ribbons. (**C**) Structural alignment of *Tb*TRF Myb domain (light blue) with that of human TRF1 (light yellow, PDB ID 1ITY) and TRF2 (gold, PDB ID 1VF9). The *Tb*TRF Myb domain is the energy minimized average structure generated from the ensemble. (**D**) The hydrophobic core and the D306-H346 salt bridge in the *Tb*TRF Myb structure.

Lastly, we performed EMSA analysis using the same J-containing single-repeat DNA as a substrate. The partially purified bacteria-expressed *Tb*TRF myb domain showed a similar DNA-binding activity regardless of whether the telomeric DNA substrate contained J or not (Supplementary Figure S3B). These results confirm that the presence of J in the telomeric DNA does not affect its interaction with the *Tb*TRF Myb domain *in vitro*.

To better quantify the telomeric DNA-binding activity of *Tb*TRF *in vivo*, we performed a ChIP analysis in BF cells treated with or without DMOG, a cell-permeable inhibitor of dioxygenase (51). It has been shown that treating BF *T. brucei* cells with 0.5 mM DMOG in DMSO for 6 days resulted in 80% of decrease in cellular J (52). We performed *Tb*TRF ChIP in the presence and absence of DMOG and found that similar amount of *Tb*TRF was associated with the telomeric DNA under both conditions (Figure 3B). To confirm that treating cells with DMOG removed most telomeric J, we performed a Southern analysis. It has been shown that the active *VSG* ES does not contain J, while silent ESs do (29), and J modification prevents PstI digestion (53,54). Indeed, we found that in the VSG2-expressor, the active *VSG2* gene was fully digested by PstI (Supplementary Figure S3C, S3D). However, in the VSG9-expressor, the same *VSG2* gene, now silent, was only partially digested by PstI (Supplementary Figure S3C, S3D). Treating cells with 0.5 mM DMOG for 6 days allowed the silent *VSG2* locus to be fully digested with PstI, indicating that DMOG successfully removed the J modification. Treating cells with DMSO (as a control) did not have any effect on J (Supplementary Figure S3C). In addition, as expected, DMOG treatment did not affect cell growth (Supplementary Figure S3E), because J is not essential for *T. brucei* growth (55). Therefore, J modification does not affect the telomeric DNA-binding activity of *Tb*TRF.

Perturbing the *Tb*TRF Myb domain significantly decreases its DNA-binding activity

NMR titration experiments were performed to identify *Tb*TRF Myb residues critical for DNA binding. A double-repeat DNA oligo with sequence 5′ GGCGCGCTTAGGGTTAGGGTTACCGCCCG 3′ was titrated into ^{15}N-labeled *Tb*TRF Myb and the resulting HSQC spectrum was compared to that of protein alone (Figure 4A). Overall the DNA-titrated HSQC spectrum showed significant difference as compared to the *Tb*TRF Myb-only spectrum, confirming that there was a direct interaction between *Tb*TRF Myb and the double-repeat oligo. The severe broadening of many cross peaks in the titrated spectrum was probably due to the large size of the *Tb*TRF Myb–DNA complex formed (~80 kDa with two *Tb*TRF Myb domains associated with the double-repeat DNA oligo).

While the broadening hindered our effort to pinpoint key DNA-binding residues, we proceeded to generate a model of *Tb*TRF Myb in complex with the telomeric DNA using the human TRF1 Myb-DNA structure as a reference (PDB ID 1W0T) (56). *Tb*TRF Myb was aligned onto hu-

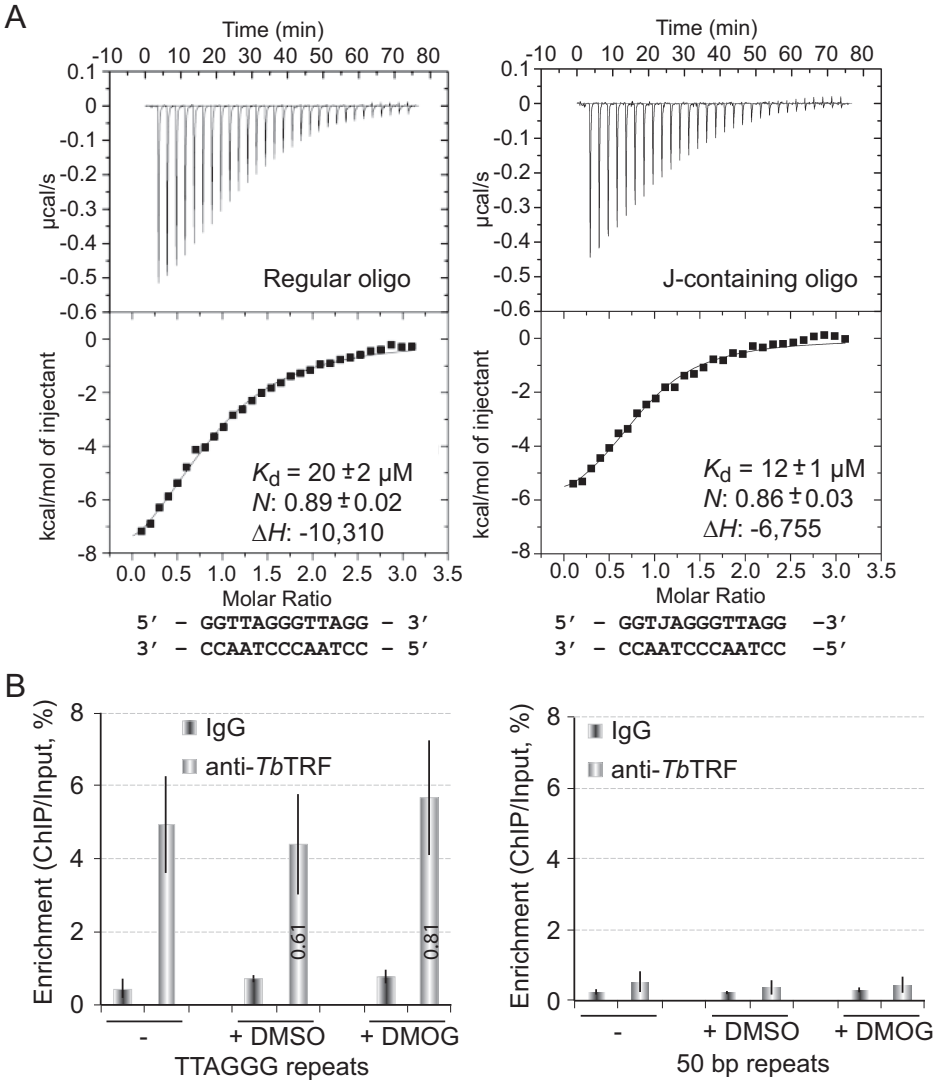

Figure 3. Characterization of *Tb*TRF binding to telomeric DNA. (**A**) ITC-based measurement of *Tb*TRF Myb–DNA interaction using regular (left) and J-containing oligo (right). Each measurement was repeated three times. Values of binding affinity (K_d), stoichiometry (N) and binding enthalpy (ΔH) with standard deviation are shown. (**B**) J does not influence the binding of *Tb*TRF on telomeric DNA *in vivo*. ChIP was performed using *Tb*TRF antibody (21) in cells grown in normal medium, medium with Dimethyl sulfoxide (DMSO) or medium with 0.5 mM Dimethyloxalylglycine (DMOG) dissolved in DMSO. Southern analyses using the TTAGGG repeat (left) or the 50 bp repeat (right) probe were performed to hybridize the ChIP products. Southern blots were exposed to phosphorimager screens and the percentage of enrichment was calculated by dividing the ChIP signal by the input signal. Average values were calculated from at least three independent experiments.

man TRF1 Myb with its third helix inserted into the major groove of telomeric DNA, mimicking the canonical Myb–DNA-binding mode (Figure 4B). In this model, the conserved R348 was well positioned to make sequence-specific contact with the G-C triplet in the telomeric repeat. Its correspondence in human TRF1, R425, has been shown to make similar sequence-specific interactions with the telomeric DNA substrate (49). Furthermore, our model showed that Q320 and Q321, two *Tb*TRF Myb-specific residues not highly conserved in the mammalian system, were also in close proximity to make contact with the sugar-phosphate backbone of DNA substrate. Based on our NMR data and modeling observations, we selected these residues (Q320, Q321 and R348) and three additional residues (R298, H346 and R352) for structure-based biochemical and functional studies. H346 is included because the salt bridge interaction it forms with D306 as shown by the NMR structure could play an essential role in stabilizing the folding of *Tb*TRF Myb and facilitating its DNA-binding activity. R298 and R352 were also included because the flexible N- and C-terminal loops have been shown to contact DNA substrates by previous studies (49), although our model cannot precisely confirm this.

Additionally we also constructed a model of the *Tb*TRF Myb domain in complex with the J-containing telomeric DNA (Figure 4C). The J-base was 'grafted' onto the *Tb*TRF Myb–DNA model by superimposing a J-containing oligo (PDB ID 308D) onto the existing regular DNA in the model. The base J replacing the T in the TTAGGG strand was located on the surface of the

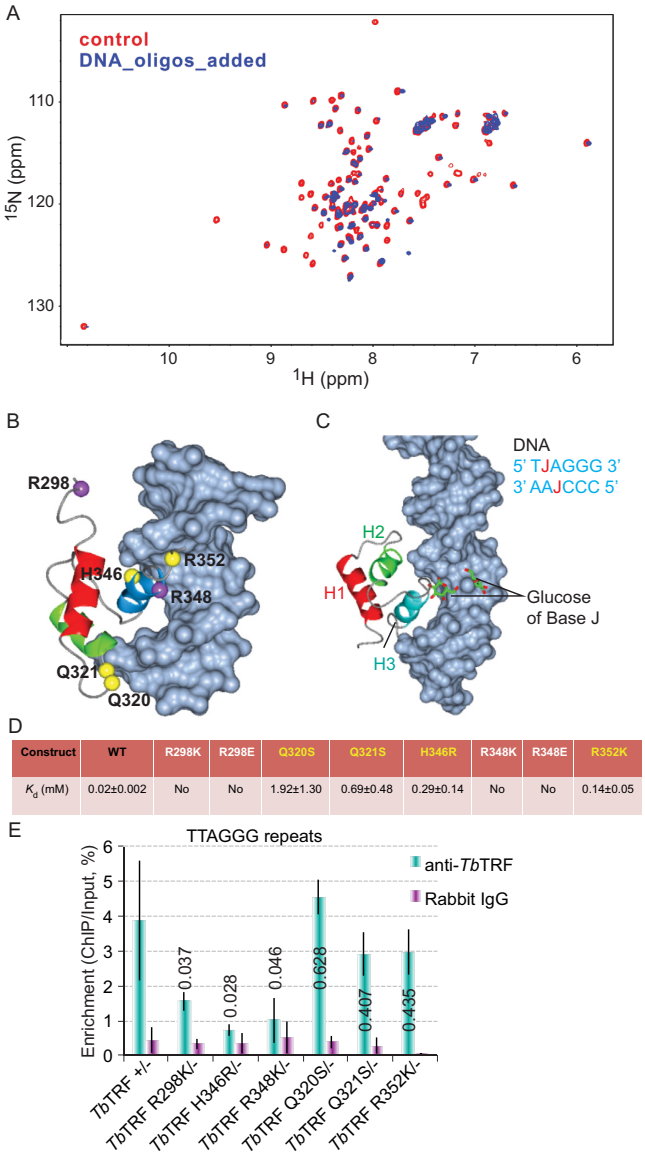

Construct	WT	R298K	R298E	Q320S	Q321S	H346R	R348K	R348E	R352K
K_d (mM)	0.02±0.002	No	No	1.92±1.30	0.69±0.48	0.29±0.14	No	No	0.14±0.05

Figure 4. Key DNA-binding residues within *Tb*TRF Myb domain. (**A**) Superposition plot of the ^{1}H–^{15}N HSQC spectra of *Tb*TRF alone and *Tb*TRF titrated with a double-repeat DNA oligo pair in 1:0.5 molar ratio. (**B**) Model of *Tb*TRF Myb domain bound to telomeric DNA generated by superimposing *Tb*TRF Myb onto human TRF1 Myb–DNA complex structure (PDB ID 1IV6). (**C**) Model of *Tb*TRF Myb bound to a J-containing DNA. The J-DNA (PDB ID 308D) is superimposed onto regular DNA in the *Tb*TRF Myb–DNA complex structure of (B). (**D**) Binding affinity (K_d) of WT and mutant *Tb*TRF Myb domain with a duplex telomeric oligo of sequence 5′ GGCGCGCTTAGGGTTAGGGTTACCGCCCG 3′ as measured by ITC. (**E**) ChIP analyses of *Tb*TRF myb point mutants. ChIP experiments were performed using *Tb*TRF antibody (21) or normal rabbit immunoglobulin G in cells expressing the *Tb*TRF Myb point mutant as the only *Tb*TRF allele. Southern hybridizations were performed using the TTAGGG repeat probe or the 50 bp repeat probe as a control (Supplementary Figure S5C). Southern blots were exposed to a phosphorimager screen and signal intensities were quantified. The percentage of enrichment was calculated by dividing the ChIP signal by the input signal. The average was calculated from at least three independent experiments. *P* values (unpaired *t* tests) of *Tb*TRF ChIP result between each mutant and *Tb*TRF +/- are listed on each column.

DNA major groove and was in the vicinity of the loop connecting the second and third helix but sufficiently away from the most critical DNA-binding residues on the third helix. The base J replacing the T in the complementary AATCCC strand was positioned completely away from the Myb-binding site and unlikely to exert any influence. Thus, our model supports our binding studies that the presence of J is unlikely to exert any direct influence on the DNA-binding activity of the *Tb*TRF Myb domain.

Focusing on the six residues identified by NMR titration studies and supported by our structural model, we generated a series of mutant *Tb*TRF Myb constructs (Figure 4D). EMSA (Supplementary Figure S4A) and ITC experiments (Supplementary Figure S4B) were performed to characterize the DNA-binding affinities of these mutants *in vitro*. Indeed, mutations targeting the highly conserved R348 such as R348E and a milder perturbation of R348K completely abolished the DNA binding. Similar effect was also observed for the N-terminal R298 mutations, suggesting that R298 directly participates in DNA binding. However, mutations targeting the *Tb*TRF Myb-specific residues such as Q320, Q321 and H346 did not abolish the DNA binding, although the binding was significantly weakened.

To further characterize the mutant *Tb*TRF DNA-binding activity *in vivo*, we introduced these point mutations into *T. brucei* cells. In the *Tb*TRF single knockout (sko) background, we replaced the remaining endogenous WT *Tb*TRF allele with the mutant *Tb*TRF allele carrying an N-terminal Ty1 tag. We could not obtain *T. brucei* strains that only expressed the *Tb*TRF R298E or *Tb*TRF R348E mutant, suggesting that these strong mutational perturbations completely abolished the *in vivo* telomeric DNA-binding activity of *Tb*TRF and were not viable. All other *Tb*TRF mutants were expressed equally in western analysis at a level similar to that in *Tb*TRF sko cells (Supplementary Figure S5A), and sequencing analysis confirmed the mutation in each mutant strain. Among *Tb*TRF Myb mutants, H346R exhibited a mild slow growth phenotype, while R298K and R348K had a slow growth phenotype that is even milder (Supplementary Figure S5B).

We performed *Tb*TRF ChIP analysis in the *Tb*TRF mutant strains. H346R had the weakest telomeric DNA-binding activity, while R298K and R348K also exhibited weaker than WT telomeric DNA-binding activities (Figure 4E, Supplementary Figure S5C), and the differences between these three mutants and WT *Tb*TRF are significant. In contrast, Q320S, Q321S and R352K mutants are associated with the telomeric DNA at similar levels to that of the WT (Figure 4E, Supplementary Figure S5C), indicating that the telomeric DNA-binding activities in these *Tb*TRF Myb mutants were not significantly affected *in vivo*.

To examine whether *VSG* silencing is affected in *Tb*TRF myb mutants, we performed qRT-PCR to estimate the steady-state mRNA levels of several ES-linked *VSGs* and several control genes including *Tb*TERT, *Tb*RPS15 and rRNA in *Tb*TRF mutants and sko cells. In most cases, we did not observe higher *VSG* mRNA levels in *Tb*TRF mutants than in sko cells except that elevated *VSG3* and *VSG13* mRNA levels were detected in H346R/- and R348K/- cells, respectively (Supplementary Figure S5D), suggesting that

decreasing the DNA-binding activity of *Tb*TRF did not affect *VSG* silencing globally.

*Tb*TRF Myb domain mutants with weakened DNA binding show increased VSG switching frequencies

We found that a transient depletion of *Tb*TRF led to an increased VSG switching frequency. To further test whether the telomeric DNA-binding activity of *Tb*TRF is essential for VSG switching regulation, we introduced *Tb*TRF Myb mutants that significantly reduced the telomere DNA-binding activity (H346R, R298K and R348K) in HSTB261 cells and deleted the remaining WT *Tb*TRF allele. As a control, we also introduced the Q320S mutant that did not affect *Tb*TRF DNA-binding activity into HSTB261. Western analysis confirmed the expression of the *Tb*TRF mutants in these cells (Supplementary Figure S5E). Southern and PCR analyses also confirmed the *Tb*TRF genotype, and sequencing analysis verified each mutant (data not shown).

We performed the VSG switching analysis in *Tb*TRF myb domain mutants using MACS to enrich the VSG switchers. We found that *Tb*TRF sko strain exhibited a similar VSG switching frequency as the S/v cells (Figures 1C and 5A), indicating that a single allele of *Tb*TRF was sufficient for its function in VSG switching regulation. Interestingly, S/H346R had a significantly increased (3.3-fold) VSG switching frequency than S/TRF sko (Figure 5A). In addition, S/R298K and S/R348K cells showed a mild but significant increase in VSG switching frequency (1.6 fold) (Figure 5A). In contrast, S/Q320S behaved similarly as S/TRF sko cells. Therefore, the H346R mutant that significantly reduced the association of *Tb*TRF with the telomeric DNA *in vivo* led to significantly more VSG switching. R298K and R348K mutants that mildly affected the *in vivo* DNA-binding activity also mildly increased VSG switching frequency. While the Q320S mutant that did not affect DNA binding *in vivo* did not affect VSG switching, either, indicating that the telomere DNA-binding activity is critical for the role of *Tb*TRF in VSG switching regulation.

We further characterized the VSG switching mechanisms in S/TRF sko and *Tb*TRF myb mutants. Similar to S/v cells, S/TRF sko cells had predominantly *VSG* GC events (84%) and a considerable percentage of ES GC/ES loss + *in situ* events (14%). In *Tb*TRF mutants that exhibited more frequent VSG switching, we observed a decreased percentage of *VSG* GC events (48–56%) and an increased percentage of ES GC/ES loss + *in situ* events (40–48%), which was similar to that in *Tb*TRF-depleted cells, although the effects were to a lesser degree (Figures 1D and 5B). In addition, we observed an increase in *in situ* switchers in *Tb*TRF mutants (from 0% in sko cells to 1.8–5.3% in *Tb*TRF mutants), which is similar to induced S/TRFi cells (Figure 1D). Therefore, the DNA-binding activity of *Tb*TRF is important for its function in VSG switching regulation.

To verify that VSG switchers were correctly assigned with corresponding switching mechanisms, we randomly picked switchers from various *Tb*TRF genetic backgrounds and performed PFGE and Southern analyses using *VSG2*, *BSD* and the newly activated *VSG* probes. Supplementary Figure S6 shows that all tested *VSG* switchers were correctly classified.

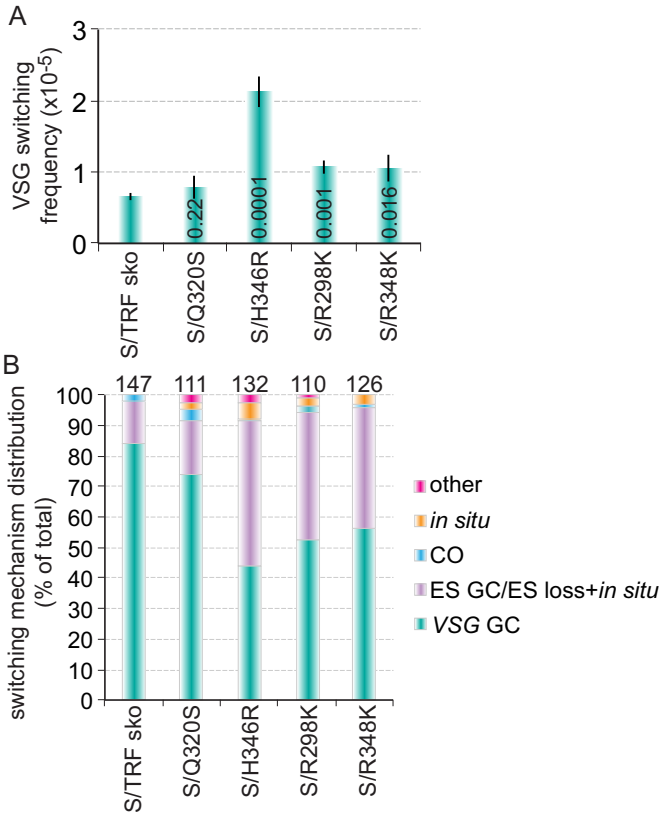

Figure 5. *Tb*TRF myb mutations that decreased the telomere DNA-binding activity also increased the VSG switching frequencies. (**A**) VSG switching frequencies in S/TRF sko and S/TRF mutants. Average values were calculated from at least three independent experiments. *P* values (unpaired *t* tests) comparing S/TRF sko and S/TRF mutants are indicated on each column. (**B**) VSG switching mechanism distribution in S/TRF sko and S/TRF mutants. The total number of switchers characterized is indicated above each column.

DISCUSSION

TRF is an essential telomeric protein conserved among a number of species from the *T. brucei* protozoan to human. In mammalian cells, TRF1 and TRF2 are two key components of the Shelterin complex that protects the chromosome end (57). Removal of TRF2 from telomeres led to ATM/p53-dependent ligase IV-mediated NHEJ of telomere ends (58–60). Removal of TRF1 from telomeres led to telomere elongation (61) and fragile telomeres (62). Both TRF1 and TRF2 contain a highly conserved C-terminal Myb domain that directly binds to the telomeric DNA, which enables TRFs to serve as architectural factors and to nucleate the Shelterin complex at the telomere (63). Structural analysis of mammalian TRF myb domains revealed that these structural modules use a conserved helix-turn-helix motif for specific binding to the TTAGGG telomeric sequence (49,56).

T. brucei is a protozoan parasite that undergoes antigenic variation through VSG switching to evade the host immune response (2). Because the repertoire of over 2000 *VSG* genes in *T. brucei* are located at subtelomeres (4), the telomere structure and associated proteins have long been speculated to play a role in VSG switching regulation, although limited

data have been reported to support this hypothesis (12,20). *Tb*TRF is the first telomere protein identified and found to be essential for maintaining the telomere terminal structure in *T. brucei* (21). The role of *Tb*TRF in VSG switching has not been investigated, although it is not required for subtelomeric *VSG* silencing (18).

Here we have conducted structural and functional studies to delineate the role of *Tb*TRF and its Myb domain in VSG switching. First, we found that a transient depletion of *Tb*TRF led to significantly more VSG switchers and most of these arose from ES GC/ES loss + *in situ* events. This confirms a definitive role of *Tb*TRF in suppression of VSG switching. Although a transient depletion of *Tb*TRF led to a growth arrest, this arrest is short-term and fully reversible, excluding the possibility that the observed more frequent VSG switching is a 'death phenotype'. RNAi has been used to show that several essential proteins are important in regulation of VSG switching through apparently different mechanisms (12,35,64,65). Furthermore, a simple slow growth is not expected to result in more frequent VSG switching, because deletion of *Tb*MRE11 led to significantly slow growth, but did not affect VSG switching (66).

Second, our structural data show that the *Tb*TRF Myb domain adopts the canonical helix-turn-helix DNA-binding motif shared by all Myb domains. The three core helices are tightly packed together by a cluster of hydrophobic residues. This core region superimposes very well with mammalian TRF1/2 Myb domain structures, suggesting a highly conserved structural module for sequence-specific binding to telomeric DNA repeats. However, the loops connecting the three helices and both the N- and C-termini of Myb region are highly flexible, with little sequence identity between *Tb*TRF and mammalian TRF1/2.

Furthermore, our *in vitro* data show that the *Tb*TRF Myb domain binds to telomeric sequences containing the bulky J-base with similar affinity as to normal telomeric sequences. Structure-based modeling suggests that although J is a bulky modification, it is not located at the interface of DNA and *Tb*TRF interaction. Thus, J is unlikely to affect *Tb*TRF binding. Our *in vivo* ChIP analysis further confirmed that *Tb*TRF associated with the telomeric DNA at equal efficiency whether the substrate contained J or not.

There have been no reports on whether mammalian TRF1/2 can bind to J-containing telomeric DNA. A previous study showed that human TRF1 could be expressed in PF *T. brucei* cells and was located at the telomere that does not have J modification (67). However, human TRF1, when expressed in BF *T. brucei* cells where the DNA is modified by J, is not located at the telomere (67). Presumably, the presence of J in BF telomeres interfered with efficient binding of human TRF1, although the possibility that other telomere factors are involved in such reduced TRF1 binding cannot be ruled out. Further studies, such as *in vitro* measurement of the binding affinity of mammalian TRF1/2 Myb to J-DNA and *in vivo* ChIP assays, are needed to fully address this question.

We generated a series of structure-based mutations within the *Tb*TRF Myb domain to abolish or weaken its DNA-binding affinity. Three assays, including the *in vitro* EMSA and ITC, together with the *in vivo* ChIP assay, were used to characterize the effects of individual mutations on the DNA-binding activity of *Tb*TRF. VSG switching assays were also carried out to correlate the DNA-binding affinity of these *Tb*TRF mutations to their VSG regulation function. For all mutations except H346R (discussed below), results from all these assays are consistent or at least show the same trend of effects. Specifically, R298E and R348E abolished *in vitro* DNA-binding activity, and we could not obtain any cells expressing these mutant alleles, suggesting that they also abolish DNA binding *in vivo*. R298K and R348K abolished *in vitro* DNA-binding activity and showed significantly reduced telomere association and increased VSG switching *in vivo,* while Q320S, Q321S and R348K only weakened *in vitro* DNA-binding activity and exhibited subtle and insignificant effects on their *in vivo* telomere association and VSG switching.

Therefore, all tested Myb mutants except H346R showed milder effects *in vivo* than *in vitro*. Such mild *in vivo* effect is likely due to different *Tb*TRF constructs used in *in vitro* and *in vivo* methods. *Tb*TRF homodimerizes through its TRFH domain, and this dimerization is critical for its *in vivo* telomere DNA-binding activity (21), because at least two Myb domains are required for efficient DNA recognition (68). In addition, *Tb*TRF interacts with other telomere proteins in live cells (12,18), which may also influence its *in vivo* telomere DNA-binding activity. Our *in vitro* studies were performed with the Myb domain alone, which is not expected to dimerize, while our *in vivo* assays were performed with full-length *Tb*TRF proteins that are capable of dimerization. Therefore, it is possible that dimerization of *Tb*TRF mutants, as well as its interaction with other telomeric factors, may serve to recover some of the mutants' DNA-binding activity *in vivo*.

H346R is unique among the tested mutants, as it showed a stronger phenotype *in vivo* than *in vitro*. Its *in vitro* DNA-binding affinity is stronger than that of R298K and R348K (weakened versus abolished), yet its ChIP enrichment is weaker and its VSG switching frequency higher than the latter two mutants. This is likely because of the unique role of H346 when compared to other residues. As shown by our NMR data, H346 is critical for the proper folding of *Tb*TRF Myb domain, although it does not directly interact with the telomeric DNA. Thus, the stronger *in vivo* effect of H346R was probably caused by the loss of proper folding of full-length *Tb*TRF when the Myb domain structure was compromised.

In summary, the *Tb*TRF Myb mutations that abolished (R298K and R348K) or weakened (H346R) DNA binding in *in vitro* analyses led to reduced *in vivo* DNA binding when analyzed by ChIP, enhanced VSG switching by 1.6–3.3 fold and increased the proportion of ES GC/ES loss + *in situ* switchers, demonstrating that the function of *Tb*TRF in VSG switching regulation depends on the structural integrity and telomere DNA-binding activity of its Myb domain.

*Tb*TRF plays an essential role in maintaining the telomere terminal structure and is a functional homolog of mammalian TRF2 (21). Similar to loss of TRF2 (58–60), loss of *Tb*TRF could result in telomere fusions and subsequent breakage-fusion-bridge cycle, which often result in large terminal chromosome deletions (69). Since loss of VSG expression is lethal for *T. brucei* cells (70), it is possible that

only switchers that express a different VSG can survive the *Tb*TRF-depletion-induced loss of the active *VSG* gene. However, chromosome end fusions have not been detected in *T. brucei*. It is unknown whether NHEJ exists in this protozoan, because no DNA Ligase IV homolog has been identified in *T. brucei* (71), although Ku homologs have been identified (72,73).

Recent studies showed that increased DNA damages in the active ES lead to greatly increased VSG switching frequencies (10,74), and damages downstream of the active *VSG* gene often lead to ES loss (10). It is possible that *Tb*TRF has a conserved function in telomere DNA replication as human TRF proteins (62,75). In this case, loss of *Tb*TRF could lead to stalled DNA replication forks in telomere repeats, which would cause increased damages at telomeres that contribute to increased VSG switching. Additional investigations are necessary to examine whether depletion of *Tb*TRF would lead to elevated DNA damages at telomeres and subtelomeres.

*Tb*TRF plays an important role in VSG switching regulation, a critical aspect of antigenic variation in *T. brucei*. The function of *Tb*TRF is different from that of *Tb*RAP1, which is a *Tb*TRF-interacting factor and is essential for subtelomeric ES-linked and metacyclic *VSG* silencing in both BF and PF *T. brucei* cells (18,19). Therefore, although *Tb*TRF interacts with *Tb*RAP1 (18), these two telomere proteins appear to have independent functions in antigenic variation regulation. In contrast, depletion of another telomere protein, *Tb*TIF2, also leads to more frequent VSG switching and more ES GC/ES loss + *in situ* switching events (12). Because *Tb*TRF is the telomere DNA-binding protein and *Tb*TIF2 is presumably recruited to the telomere by interacting with *Tb*TRF, it is possible that depletion of *Tb*TRF resulted in removal of *Tb*TIF2 from the telomere, which in turn leads to elevated VSG switching frequency (12). Further investigations of how *Tb*TIF2 is recruited to the telomere will help answer this question. *Tb*TRF appears to interact with *Tb*TIF2 more strongly than with *Tb*RAP1 in both yeast 2-hybrid and co-IP experiments (12,18). Hence, it is likely that *Tb*TRF and *Tb*TIF2 function in the same pathway in regulating VSG switching. However, it is necessary to examine VSG switching frequencies and mechanisms in cells depleted of both *Tb*TRF and *Tb*TIF2 to determine definitively whether the two proteins work in the same pathway.

SUPPLEMENTARY DATA

Supplementary Data are available at NAR Online.

ACKNOWLEDGMENTS

We thank Dr Hee-Sook Kim and Dr George A. M. Cross for sending us the HSTB261 cells. The Li and Zhao lab members are thanked for their comments on the manuscript. Sandhu Ranjodh and Fei Ye contributed equally.

FUNDING

National Institute of Health [AI066095, PI to B.L.]; Hong Kong Research Grants Council [PolyU5639/09M, PolyU5644/10M, PolyU5640/11M, HKUST6/CRF/10 and AoE/M-09/12, PI to Y.Z.]; Research Committee of the Hong Kong Polytechnic University; National Natural Science Foundation of China [31200563, PI to X.L.]. Funding for open access charge: National Institute of Health [AI066095, PI to B.L.]; Hong Kong Research Grants Council [PolyU5644/10M, PI to Y.Z.].
Conflict of interest statement. None declared.

REFERENCES

1. Babokhov,P., Sanyaolu,A.O., Oyibo,W.A., Fagbenro-Beyioku,A.F. and Iriemenam,N.C. (2013) A current analysis of chemotherapy strategies for the treatment of human African trypanosomiasis. *Pathog. Glob. Health*, **107**, 242–252.
2. Barry,J.D. and McCulloch,R. (2001) Antigenic variation in trypanosomes: enhanced phenotypic variation in a eukaryotic parasite. *Adv. Parasitol.*, **49**, 1–70.
3. Berriman,M., Ghedin,E., Hertz-Fowler,C., Blandin,G., Renauld,H., Bartholomeu,D.C., Lennard,N.J., Caler,E., Hamlin,N.E.,, Haas,B. *et al.* (2005) The genome of the African trypanosome *Trypanosoma brucei*. *Science*, **309**, 416–422.
4. Cross,G.A.M., Kim,H.S. and Wickstead,B. (2014) Capturing the variant surface glycoprotein repertoire (the VSGnome) of *Trypanosoma brucei* Lister 427. *Mol. Biochem. Parasitol.*, **195**, 59–73.
5. Gunzl,A., Bruderer,T., Laufer,G., Schimanski,B., Tu,L.C., Chung,H.M., Lee,P.T. and Lee,M.G. (2003) RNA polymerase I transcribes procyclin genes and variant surface glycoprotein gene expression sites in *Trypanosoma brucei*. *Eukaryot. Cell*, **2**, 542–551.
6. de Lange,T. and Borst,P. (1982) Genomic environment of the expression-linked extra copies of genes for surface antigens of *Trypanosoma brucei* resembles the end of a chromosome. *Nature*, **299**, 451–453.
7. Hertz-Fowler,C., Figueiredo,L.M., Quail,M.A., Becker,M., Jackson,A., Bason,N., Brooks,K., Churcher,C., Fahkro,S., Goodhead,I. *et al.* (2008) Telomeric expression sites are highly conserved in *Trypanosoma brucei*. *PLoS One*, **3**, e3527.
8. Crozatier,M., van der Ploeg,L.H., Johnson,P.J., Gommers-Ampt,J. and Borst,P. (1990) Structure of a telomeric expression site for variant specific surface antigens in *Trypanosoma brucei*. *Mol. Biochem. Parasitol.*, **42**, 1–12.
9. Morrison,L.J., Marcello,L. and McCulloch,R. (2009) Antigenic variation in the African trypanosome: molecular mechanisms and phenotypic complexity. *Cell. Microbiol.*, **11**, 1724–1734.
10. Glover,L., Alsford,S. and Horn,D. (2013) DNA break site at fragile subtelomeres determines probability and mechanism of antigenic variation in African trypanosomes. *PLoS Pathog.*, **9**, e1003260.
11. Kim,H.S. and Cross,G.A.M. (2011) Identification of *Trypanosoma brucei* RMI1/BLAP75 homologue and its roles in antigenic variation. *PLoS One*, **6**, e25313.
12. Jehi,S.E., Wu,F. and Li,B. (2014) *Trypanosoma brucei* TIF2 suppresses VSG switching by maintaining subtelomere integrity. *Cell Res.*, **24**, 870–885.
13. Proudfoot,C. and McCulloch,R. (2005) Distinct roles for two RAD51-related genes in *Trypanosoma brucei* antigenic variation. *Nucleic Acids Res.*, **33**, 6906–6919.
14. McCulloch,R. and Barry,J.D. (1999) A role for RAD51 and homologous recombination in *Trypanosoma brucei* antigenic variation. *Genes Dev.*, **13**, 2875–2888.
15. Hartley,C.L. and McCulloch,R. (2008) *Trypanosoma brucei* BRCA2 acts in antigenic variation and has undergone a recent expansion in BRC repeat number that is important during homologous recombination. *Mol. Microbiol.*, **68**, 1237–1251.
16. Kim,H.S. and Cross,G.A.M. (2010) TOPO3alpha influences antigenic variation by monitoring expression-site-associated *VSG* switching in *Trypanosoma brucei*. *PLoS Pathog.*, **6**, e1000992.
17. Dreesen,O., Li,B. and Cross,G.A.M. (2007) Telomere structure and function in trypanosomes: a proposal. *Nat. Rev. Microbiol.*, **5**, 70–75.
18. Yang,X., Figueiredo,L.M., Espinal,A., Okubo,E. and Li,B. (2009) RAP1 is essential for silencing telomeric variant surface glycoprotein genes in *Trypanosoma brucei*. *Cell*, **137**, 99–109.

19. Pandya,U.M., Sandhu,R. and Li,B. (2013) Silencing subtelomeric VSGs by *Trypanosoma brucei* RAP1 at the insect stage involves chromatin structure changes. *Nucleic Acids Res.*, **41**, 7673–7682.
20. Hovel-Miner,G.A., Boothroyd,C.E., Mugnier,M., Dreesen,O., Cross,G.A.M. and Papavasiliou,F.N. (2012) Telomere length affects the frequency and mechanism of antigenic variation in *Trypanosoma brucei*. *PLoS Pathog.*, **8**, e1002900.
21. Li,B., Espinal,A. and Cross,G.A.M. (2005) Trypanosome telomeres are protected by a homologue of mammalian TRF2. *Mol. Cell Biol.*, **25**, 5011–5021.
22. Chen,Y., Yang,Y., van Overbeek,M., Donigian,J.R., Baciu,P., de Lange,T. and Lei,M. (2008) A shared docking motif in TRF1 and TRF2 used for differential recruitment of telomeric proteins. *Science*, **319**, 1092–1096.
23. Bianchi,A., Smith,S., Chong,L., Elias,P. and de Lange,T. (1997) TRF1 is a dimer and bends telomeric DNA. *EMBO J.*, **16**, 1785–1794.
24. Bianchi,A., Stansel,R.M., Fairall,L., Griffith,J.D., Rhodes,D. and de Lange,T. (1999) TRF1 binds a bipartite telomeric site with extreme spatial flexibility. *EMBO J.*, **18**, 5735–5744.
25. Broccoli,D., Smogorzewska,A., Chong,L. and de Lange,T. (1997) Human telomeres contain two distinct Myb-related proteins, TRF1 and TRF2. *Nat. Genet.*, **17**, 231–235.
26. Gommers-Ampt,J., Lutgerink,J. and Borst,P. (1991) A novel DNA nucleotide in *Trypanosoma brucei* only present in the mammalian phase of the life-cycle. *Nucleic Acids Res.*, **19**, 1745–1751.
27. Gommers-Ampt,J.H., Van Leeuwen,F., de Beer,A.L., Vliegenthart,J.F., Dizdaroglu,M., Kowalak,J.A., Crain,P.F. and Borst,P. (1993) beta-D-glucosyl-hydroxymethyluracil: a novel modified base present in the DNA of the parasitic protozoan *T. brucei*. *Cell*, **75**, 1129–1136.
28. van Leeuwen,F., Wijsman,E.R., Kuyl-Yeheskiely,E., van der Marel,G.A., van Boom,J.H. and Borst,P. (1996) The telomeric GGGTAA repeats of *Trypanosoma brucei* contain the hypermodified base J in both strands. *Nucleic Acids Res.*, **24**, 2476–2482.
29. van Leeuwen,F., Wijsman,E.R., Kieft,R., van der Marel,G.A., van Boom,J.H. and Borst,P. (1997) Localization of the modified base J in telomeric VSG gene expression sites of *Trypanosoma brucei*. *Genes Dev.*, **11**, 3232–3241.
30. van Leeuwen,F., Kieft,R., Cross,M. and Borst,P. (2000) Tandemly repeated DNA is a target for the partial replacement of thymine by beta-D-glucosyl-hydroxymethyluracil in *Trypanosoma brucei*. *Mol. Biochem. Parasitol.*, **109**, 133–145.
31. Cliffe,L.J., Siegel,T.N., Marshall,M., Cross,G.A. and Sabatini,R. (2010) Two thymidine hydroxylases differentially regulate the formation of glucosylated DNA at regions flanking polymerase II polycistronic transcription units throughout the genome of *Trypanosoma brucei*. *Nucleic Acids Res.*, **38**, 3923–3935.
32. Reynolds,D., Cliffe,L., Forstner,K.U., Hon,C.C., Siegel,T.N. and Sabatini,R. (2014) Regulation of transcription termination by glucosylated hydroxymethyluracil, base J, in *Leishmania major* and *Trypanosoma brucei*. *Nucleic Acids Res.*, **42**, 9717–9729.
33. Ekanayake,D. and Sabatini,R. (2011) Epigenetic regulation of polymerase II transcription initiation in *Trypanosoma cruzi*: modulation of nucleosome abundance, histone modification, and polymerase occupancy by O-linked thymine DNA glucosylation. *Eukaryot. Cell*, **10**, 1465–1472.
34. van Luenen,H.G., Farris,C., Jan,S., Genest,P.A., Tripathi,P., Velds,A., Kerkhoven,R.M., Nieuwland,M., Haydock,A., Ramasamy,G. *et al.* (2012) Glucosylated hydroxymethyluracil, DNA base J, prevents transcriptional readthrough in Leishmania. *Cell*, **150**, 909–921.
35. Benmerzouga,I., Concepcion-Acevedo,J., Kim,H.S., Vandoros,A.V., Cross,G.A.M., Klingbeil,M.M. and Li,B. (2013) *Trypanosoma brucei* Orc1 is essential for nuclear DNA replication and affects both *VSG* silencing and *VSG* switching. *Mol. Microbiol.*, **87**, 196–210.
36. Wuthrich,K. (1995) NMR—this other method for protein and nucleic acid structure determination. *Acta Crystallogr. D Biol. Crystallogr.*, **51**, 249–270.
37. Wider,G. (2000) Structure determination of biological macromolecules in solution using nuclear magnetic resonance spectroscopy. *Biotechniques*, **29**, 1278–1282.
38. Wishart,D. (2005) NMR spectroscopy and protein structure determination: applications to drug discovery and development. *Curr. Pharm. Biotechnol.*, **6**, 105–120.
39. Brunger,A.T., Adams,P.D., Clore,G.M., DeLano,W.L., Gros,P., Grosse-Kunstleve,R.W., Jiang,J.S., Kuszewski,J., Nilges,M., Pannu,N.S. *et al.* (1998) Crystallography & NMR system: a new software suite for macromolecular structure determination. *Acta Crystallogr. D Biol. Crystallogr.*, **54**, 905–921.
40. Potterton,L., McNicholas,S., Krissinel,E., Gruber,J., Cowtan,K., Emsley,P., Murshudov,G.N., Cohen,S., Perrakis,A. and Noble,M. (2004) Developments in the CCP4 molecular-graphics project. *Acta Crystallogr. D Biol. Crystallogr.*, **60**, 2288–2294.
41. Roselin,L.S., Lin,M.S., Lin,P.H., Chang,Y. and Chen,W.Y. (2010) Recent trends and some applications of isothermal titration calorimetry in biotechnology. *Biotechnol. J.*, **5**, 85–98.
42. Pierce,M.M., Raman,C.S. and Nall,B.T. (1999) Isothermal titration calorimetry of protein-protein interactions. *Methods*, **19**, 213–221.
43. Krell,T., Lacal,J., Garcia-Fontana,C., Silva-Jimenez,H., Rico-Jimenez,M., Lugo,A.C., Darias,J.A. and Ramos,J.L. (2014) Characterization of molecular interactions using isothermal titration calorimetry. *Methods Mol. Biol.*, **1149**, 193–203.
44. Ladbury,J.E. (2004) Application of isothermal titration calorimetry in the biological sciences: things are heating up! *Biotechniques*, **37**, 885–887.
45. Wang,Z., Morris,J.C., Drew,M.E. and Englund,P.T. (2000) Inhibition of *Trypanosoma brucei* gene expression by RNA interference using an integratable vector with opposing T7 promoters. *J. Biol. Chem.*, **275**, 40174–40179.
46. Scahill,M.D., Pastar,I. and Cross,G.A.M. (2008) CRE recombinase-based positive-negative selection systems for genetic manipulation in *Trypanosoma brucei*. *Mol. Biochem. Parasitol.*, **157**, 73–82.
47. Smith,S. and de Lange,T. (1997) TRF1, a mammalian telomeric protein. *Trends Genet.*, **13**, 21–26.
48. Oh,I.H. and Reddy,E.P. (1999) The myb gene family in cell growth, differentiation and apoptosis. *Oncogene*, **18**, 3017–3033.
49. Nishikawa,T., Okamura,H., Nagadoi,A., Koig,P., Rhodes,D. and Nishimura,Y. (2001) Solution structure of a telomeric DNA complex of human TRF1. *Structure*, **9**, 1237–1251.
50. Hanaoka,S., Nagadoi,A. and Nishimura,Y. (2005) Comparison between TRF2 and TRF1 of their telomeric DNA-bound structures and DNA-binding activities. *Protein Sci.*, **14**, 119–130.
51. Rose,N.R., McDonough,M.A., King,O.N., Kawamura,A. and Schofield,C.J. (2011) Inhibition of 2-oxoglutarate dependent oxygenases. *Chem. Soc. Rev.*, **40**, 4364–4397.
52. Cliffe,L.J., Hirsch,G., Wang,J., Ekanayake,D., Bullard,W., Hu,M., Wang,Y. and Sabatini,R. (2012) JBP1 and JBP2 proteins are Fe2+/2-oxoglutarate-dependent dioxygenases regulating hydroxylation of thymidine residues in trypanosome DNA. *J. Biol. Chem.*, **287**, 19886–19895.
53. McClelland,M., Nelson,M. and Raschke,E. (1994) Effect of site-specific modification on restriction endonucleases and DNA modification methyltransferases. *Nucleic Acids Res.*, **22**, 3640–3659.
54. Bernards,A., van Harten-Loosbroek,N. and Borst,P. (1984) Modification of telomeric DNA in *Trypanosoma brucei*; a role in antigenic variation? *Nucleic Acids Res.*, **12**, 4153–4170.
55. Cliffe,L.J., Kieft,R., Southern,T., Birkeland,S.R., Marshall,M., Sweeney,K. and Sabatini,R. (2009) JBP1 and JBP2 are two distinct thymidine hydroxylases involved in J biosynthesis in genomic DNA of African trypanosomes. *Nucleic Acids Res.*, **37**, 1452–1462.
56. Court,R., Chapman,L., Fairall,L. and Rhodes,D. (2005) How the human telomeric proteins TRF1 and TRF2 recognize telomeric DNA: a view from high-resolution crystal structures. *EMBO Rep.*, **6**, 39–45.
57. de Lange,T. (2005) Shelterin: the protein complex that shapes and safeguards human telomeres. *Genes Dev.*, **19**, 2100–2110.
58. van Steensel,B., Smogorzewska,A. and de Lange,T. (1998) TRF2 protects human telomeres from end-to-end fusions. *Cell*, **92**, 401–413.
59. Karlseder,J., Broccoli,D., Dai,Y.M., Hardy,S. and de Lange,T. (1999) p53- and ATM-dependent apoptosis induced by telomeres lacking TRF2. *Science*, **283**, 1321–1325.
60. Celli,G.B. and de Lange,T. (2005) DNA processing is not required for ATM-mediated telomere damage response after TRF2 deletion. *Nat. Cell Biol.*, **7**, 712–718.
61. van Steensel,B. and de Lange,T. (1997) Control of telomere length by the human telomeric protein TRF1. *Nature*, **385**, 740–743.

62. Sfeir,A., Kosiyatrakul,S.T., Hockemeyer,D., MacRae,S.L., Karlseder,J., Schildkraut,C.L. and de Lange,T. (2009) Mammalian telomeres resemble fragile sites and require TRF1 for efficient replication. *Cell*, **138**, 90–103.
63. Palm,W. and de Lange,T. (2008) How shelterin protects mammalian telomeres. *Annu. Rev. Genet.*, **42**, 301–334.
64. Landeira,D., Bart,J.M., Van Tyne,D. and Navarro,M. (2009) Cohesin regulates VSG monoallelic expression in trypanosomes. *J. Cell Biol.*, **186**, 243–254.
65. Povelones,M.L., Gluenz,E., Dembek,M., Gull,K. and Rudenko,G. (2012) Histone H1 plays a role in heterochromatin formation and *VSG* expression site silencing in *Trypanosoma brucei*. *PLoS Pathog.*, **8**, e1003010.
66. Robinson,N.P., McCulloch,R., Conway,C., Browitt,A. and Barry,J.D. (2002) Inactivation of Mre11 does not affect VSG gene duplication mediated by homologous recombination in *Trypanosoma brucei*. *J. Biol. Chem.*, **277**, 26185–26193.
67. Munoz-Jordan,J.L. and Cross,G.A.M. (2001) Telomere shortening and cell cycle arrest in *Trypanosoma brucei* expressing human telomeric repeat factor TRF1. *Mol. Biochem. Parasitol.*, **114**, 169–181.
68. Ogata,K., Morikawa,S., Nakamura,H., Sekikawa,A., Inoue,T., Kanai,H., Sarai,A., Ishii,S. and Nishimura,Y. (1994) Solution structure of a specific DNA complex of the Myb DNA-binding domain with cooperative recognition helices. *Cell*, **79**, 639–648.
69. Murnane,J.P. (2006) Telomeres and chromosome instability. *DNA Repair (Amst.)*, **5**, 1082–1092.
70. Smith,T.K., Vasileva,N., Gluenz,E., Terry,S., Portman,N., Kramer,S., Carrington,M., Michaeli,S., Gull,K. and Rudenko,G. (2009) Blocking variant surface glycoprotein synthesis in *Trypanosoma brucei* triggers a general arrest in translation initiation. *PLoS One*, **4**, e7532.
71. Burton,P., McBride,D.J., Wilkes,J.M., Barry,J.D. and McCulloch,R. (2007) Ku heterodimer-independent end joining in *Trypanosoma brucei* cell extracts relies upon sequence microhomology. *Eukaryot. Cell*, **6**, 1773–1781.
72. Conway,C., McCulloch,R., Ginger,M.L., Robinson,N.P., Browitt,A. and Barry,J.D. (2002) Ku is important for telomere maintenance, but not for differential expression of telomeric *VSG* genes, in African trypanosomes. *J. Biol. Chem.*, **277**, 21269–21277.
73. Janzen,C.J., Lander,F., Dreesen,O. and Cross,G.A.M. (2004) Telomere length regulation and transcriptional silencing in KU80-deficient *Trypanosoma brucei*. *Nucleic Acids Res.*, **32**, 6575–6584.
74. Boothroyd,C.E., Dreesen,O., Leonova,T., Ly,K.I., Figueiredo,L.M., Cross,G.A.M. and Papavasiliou,F.N. (2009) A yeast-endonuclease-generated DNA break induces antigenic switching in *Trypanosoma brucei*. *Nature*, **459**, 278–281.
75. Ye,J., Lenain,C., Bauwens,S., Rizzo,A., Saint-Leger,A., Poulet,A., Benarroch,D., Magdinier,F., Morere,J., Amiard,S. *et al.* (2010) TRF2 and apollo cooperate with topoisomerase 2alpha to protect human telomeres from replicative damage. *Cell*, **142**, 230–242.